

Simplified calibration procedure for a high-cycle accumulation model based on cyclic triaxial tests on 22 sands

T. Wichtmann, A. Niemunis & Th. Triantafyllidis

Institute of Soil Mechanics and Rock Mechanics, Karlsruhe Institute of Technology

ABSTRACT: A simplified calibration procedure for the material constants used in the authors' high-cycle accumulation model has been improved based on data from more than 350 drained cyclic triaxial tests performed on 22 clean quartz sands with different grain size distribution curves. The simplified method allows the estimation of a set of parameters from characteristics of the grain size distribution curve (mean grain size, coefficient of uniformity) and index quantities (minimum and maximum void ratio).

1 INTRODUCTION

The high-cycle accumulation (HCA) model proposed by Niemunis et al. (2005) predicts the accumulation of permanent deformations or the build-up of excess pore water pressure due to a cyclic loading with many cycles ($N > 10^3$) of small to intermediate strain amplitudes ($\varepsilon^{\text{ampl}} < 10^{-3}$). The model can be used for example for the prediction of permanent deformations of offshore wind power plant (OWPP) foundations (Wichtmann et al., 2010b).

The determination of the material constants of the HCA model (Wichtmann et al., 2010a) is quite laborious. Drained cyclic triaxial tests with different amplitudes, densities and average stresses are necessary. Regarding the large number of OWPPs in a wind park and the layered soil, an experimental determination of the constants for each OWPP foundation and each soil type would be tedious. Therefore, a simplified calibration procedure has been already proposed by Wichtmann et al. (2009) based on cyclic triaxial tests on eight quartz sands with different grain size distribution curves. Correlations of the HCA model constants with index properties (mean grain size d_{50} , coefficient of uniformity C_u , minimum void ratio e_{min}) have been developed for that purpose. However, some of the correlations showed a significant amount of scatter.

Therefore, 14 more grain size distribution curves with linear shape (in the semi-logarithmic scale) and with different mean grain sizes and coefficients of uniformity were tested in order to improve the correlations and to adapt them to a wider range of d_{50} - and C_u -values. The present paper reports on this effort.

2 TESTED MATERIALS AND TESTING PROCEDURES

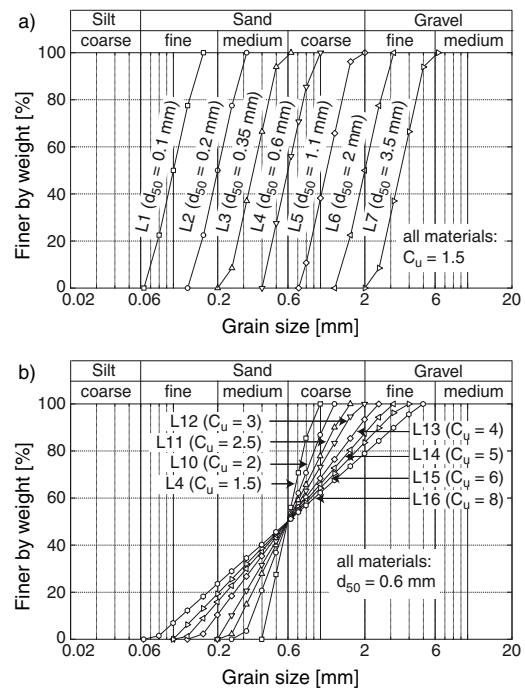


Figure 1. Tested grain size distribution curves.

The 14 tested grain size distribution curves are shown in Figure 1. They were mixed from a natural quartz sand with subangular grain shape. The sands and gravels L1 to L7 (Figure 1a) have mean grain sizes in the range $0.1 \text{ mm} \leq d_{50} \leq 3.5 \text{ mm}$ and the same coefficient of uniformity $C_u = d_{60}/d_{10} = 1.5$. The materials L4 and L10 to L16 (Figure 1b) have the same mean grain size $d_{50} = 0.6 \text{ mm}$ while C_u varies between 1.5 and 8.

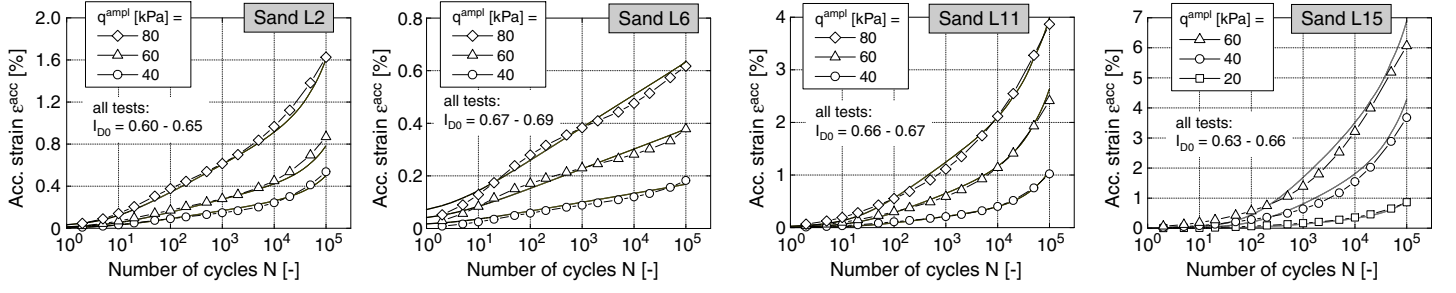


Figure 2. Accumulation curves $\varepsilon^{\text{acc}}(N)$ in tests with different stress amplitudes q^{amp} (all tests: $p^{\text{av}} = 200$ kPa, $\eta^{\text{av}} = 0.75$), thick solid curves = recalculation with HCA model.

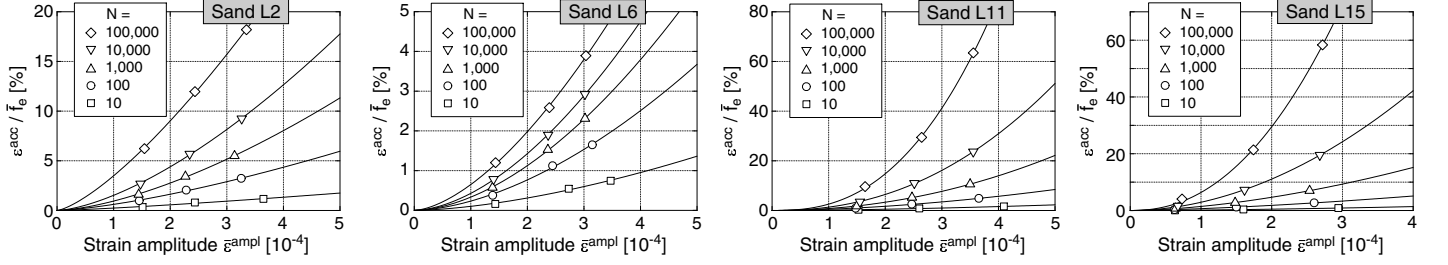


Figure 3. Accumulated strain $\varepsilon^{\text{acc}}/\bar{f}_e$ as a function of strain amplitude $\bar{\varepsilon}^{\text{amp}}$ (all tests: $p^{\text{av}} = 200$ kPa, $\eta^{\text{av}} = 0.75$).

The samples with a diameter of 10 cm and a height of 20 cm were prepared by dry air pluviation and afterwards saturated with de-aired water. They were consolidated for one hour at the average stress. Due to large deformations the first *irregular* cycle was applied with a low loading frequency of 0.01 Hz while $f = 1$ Hz was used for the subsequent 100,000 *regular* cycles. The only exception was the fine sand L1 where 2,000 or 10,000 regular cycles were tested with frequencies of 0.01 or 0.1 Hz, respectively. For each material several tests with different amplitudes, initial densities, average mean pressures p^{av} and average stress ratios $\eta^{\text{av}} = q^{\text{av}}/p^{\text{av}}$ were performed ($p = (\sigma_1 + 2\sigma_3)/3$, $q = \sigma_1 - \sigma_3$).

Since the HCA model predicts the accumulation due to the regular cycles only, the irregular cycle is not discussed in the following. The *direction* of accumulation $m = \dot{\varepsilon}^{\text{acc}}/\|\dot{\varepsilon}^{\text{acc}}\|$ (flow rule) used in the HCA model could be confirmed for all tested sands and is also not further addressed here.

3 TEST RESULTS AND DETERMINATION OF HCA MODEL CONSTANTS

The increase of the intensity of accumulation $\dot{\varepsilon}^{\text{acc}} = \|\dot{\varepsilon}^{\text{acc}}\| = \partial\varepsilon^{\text{acc}}/\partial N$ (with $\varepsilon = \sqrt{\varepsilon_1^2 + 2\varepsilon_3^2}$) with increasing stress or strain amplitude becomes clear from Figures 2 and 3. Figure 2 shows the accumulated permanent strain ε^{acc} as a function of the number of cycles N in the tests with different deviatoric stress amplitudes q^{amp} . In Figure 3 the permanent strain after different numbers of cycles is plotted versus the strain amplitude. Since in the stress-controlled tests the strain amplitude decreased slightly with N , a mean value $\bar{\varepsilon}^{\text{amp}} = 1/N \int \varepsilon^{\text{amp}}(N)dN$ over N is used

on the abscissa. On the ordinate the data is divided by the void ratio function of the HCA model in order to purify it from the influence of void ratio:

$$f_e = \frac{(C_e - e)^2}{1 + e} \frac{1 + e_{\text{max}}}{(C_e - e_{\text{max}})^2} \quad (1)$$

with the maximum void ratio e_{max} and the material constant C_e . The bar over \bar{f}_e in Figure 3 denotes that the void ratio function has been calculated with a mean value $\bar{e} = 1/N \int e(N)dN$ of void ratio. An overproportional increase of the intensity of strain accumulation with the strain amplitude can be concluded from Figure 3. The amplitude function

$$f_{\text{amp}} = (\bar{\varepsilon}^{\text{amp}}/10^{-4})^{C_{\text{amp}}} \quad (2)$$

of the HCA model has been fitted to the data shown in Figure 3 (solid curves) delivering C_{amp} . The C_{amp} -values given in column 3 of Table 1 are mean values over 100,000 cycles.

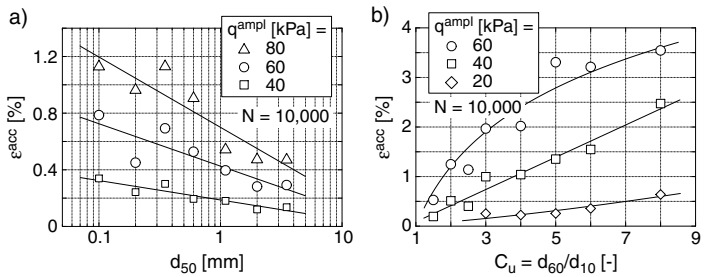


Figure 4. Accumulated strain ε^{acc} as a function of a) mean grain size d_{50} and b) coefficient of uniformity C_u .

The dependence of $\dot{\varepsilon}^{\text{acc}}$ on the grain size distribution curve is inspected in Figure 4, where the residual strain after 10,000 cycles is plotted versus d_{50} or

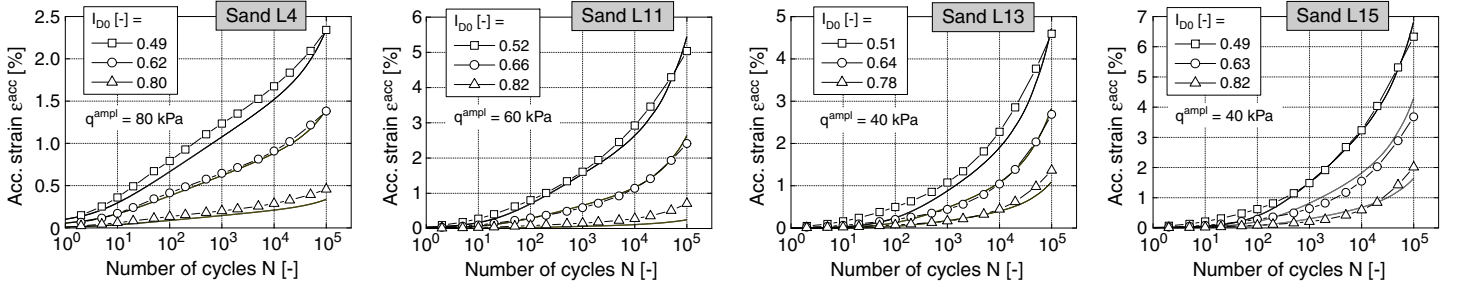


Figure 5. Accumulation curves $\varepsilon^{\text{acc}}(N)$ in tests with different initial relative densities I_{D0} (all tests: $p^{\text{av}} = 200$ kPa, $\eta^{\text{av}} = 0.75$), thick solid curves = recalculation with HCA model.

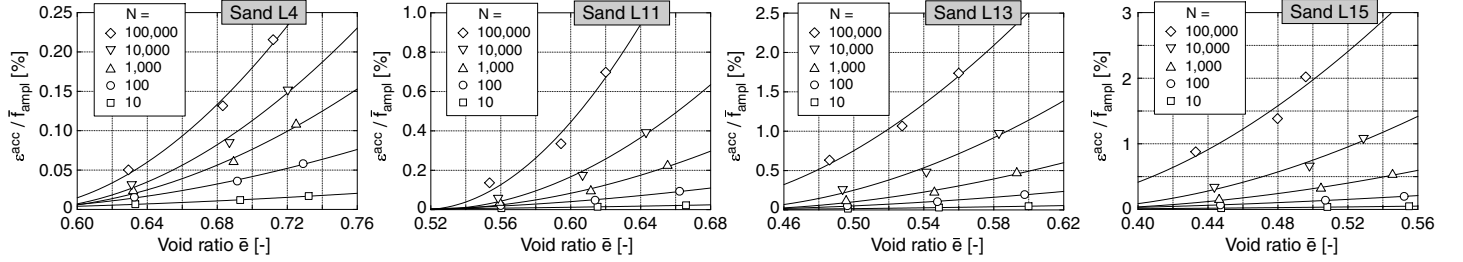


Figure 6. Accumulated strain $\varepsilon^{\text{acc}}/\bar{f}_{\text{ampl}}$ as a function of void ratio \bar{e} (all tests: $p^{\text{av}} = 200$ kPa, $\eta^{\text{av}} = 0.75$).

C_u , respectively. In accordance with Wichtmann et al. (2009) the intensity of accumulation increases with decreasing mean grain size and with increasing coefficient of uniformity.

Figures 5 and 6 demonstrate the increase of the rate of strain accumulation with increasing void ratio. While Figure 5 compares the curves $\varepsilon^{\text{acc}}(N)$ for different initial relative densities I_{D0} , Figure 6 presents the residual strain after different N -values as a function of void ratio \bar{e} . In order to purify the data from the influence of slightly different strain amplitudes, ε^{acc} has been divided by the amplitude function of the HCA model. The bar over \bar{f}_{ampl} in Figure 6 denotes that the amplitude function has been calculated with a mean value $\bar{\varepsilon}^{\text{ampl}}$ of the strain amplitude. The parameter C_e (column 4 of Table 1) was obtained from a curve-fitting of the function f_e to the data in Figure 6. Since \bar{f}_{ampl} is necessary to purify the data in Figure 6 and f_e is used on the ordinate in Figure 3, the determination of C_{ampl} and C_e has to be done by iteration.

The accumulation curves $\varepsilon^{\text{acc}}(N)$ in the tests with different average mean pressures p^{av} and with a constant average stress ratio (here $\eta^{\text{av}} = 0.75$) coincide approximately if the tests are performed with the same amplitude-pressure ratio $\zeta = q^{\text{ampl}}/p^{\text{av}}$ (Figure 7). The increase of the strain amplitude with increasing pressure for $\zeta = \text{constant}$ has been considered in Figure 8 where the residual strain has been divided by \bar{f}_{ampl} and \bar{f}_e and plotted versus p^{av} . The decrease of the intensity of accumulation with increasing average mean pressure is obvious in Figure 8. It becomes less pronounced with increasing mean grain size. The data for some sands (e.g. L15, Figure 8) indicate almost constant accumulation rates for larger pressures. Tests

with $p^{\text{av}} > 300$ kPa are planned for the future. The HCA model parameter C_p (column 5 of Table 1) was obtained from a curve-fitting of the function f_p to the data in Figure 8:

$$f_p = \exp[-C_p (p^{\text{av}}/100 \text{ kPa} - 1)] \quad (3)$$

For all tested materials the increase of the strain accumulation rate with increasing average stress ratio was confirmed. Figures 9 and 10 compare the accumulation curves $\varepsilon^{\text{acc}}(N)$ or show the residual strain as a function of the normalized average stress ratio \bar{Y}^{av} , where \bar{Y} and η are interrelated via

$$\bar{Y} = \frac{27(3 + \eta)/(3 + 2\eta)/(3 - \eta) - 9}{(9 - \sin^2 \varphi_c)/(1 - \sin^2 \varphi_c) - 9} \quad (4)$$

with critical friction angle φ_c . \bar{Y}^{av} is zero for isotropic stress conditions and equal to one on the critical state line. The HCA model parameter C_Y (column 6 of Table 1) was obtained from a curve-fitting of the function f_Y to the data in Figure 10:

$$f_Y = \exp(C_Y \bar{Y}^{\text{av}}) \quad (5)$$

The shape of the curves $\varepsilon^{\text{acc}}(N)$ can be judged from Figure 11 where the residual strain has been divided by the functions \bar{f}_{ampl} , \bar{f}_e , f_p and f_Y of the HCA model (calculated with the constants given in columns 3 to 9 of Table 1), that means it was purified from the influences of amplitude, void ratio and average stress. For uniform sands the residual strain increases almost proportional to $\ln(N)$ up to at least $N = 10^4$. At large numbers of cycles $N > 10^4$, the residual strain grew faster than proportional to $\ln(N)$ for some of the sands L1 to L7 (see e.g. L2 in Figure 11). The curves

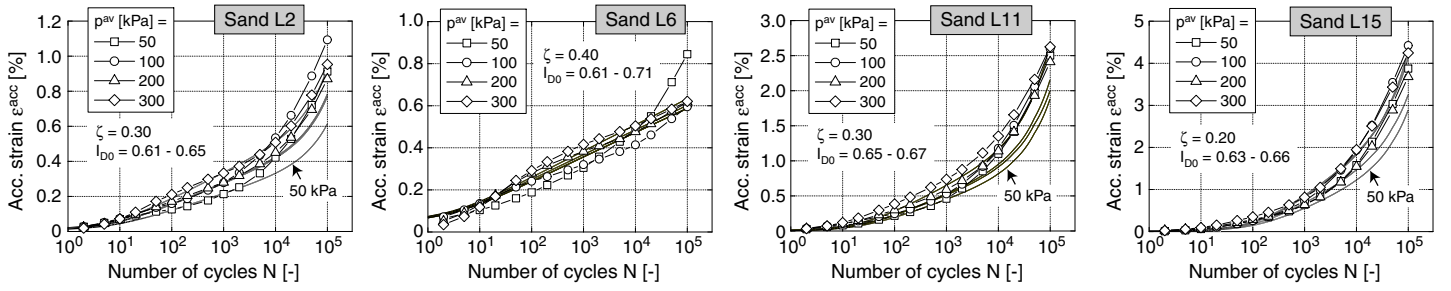


Figure 7. Accumulation curves $\varepsilon^{\text{acc}}(N)$ in tests with different average mean pressures p^{av} (all tests: $\eta^{\text{av}} = 0.75$, $\zeta = q^{\text{ampl}}/p^{\text{av}}$), thick solid curves = recalculation with HCA model.

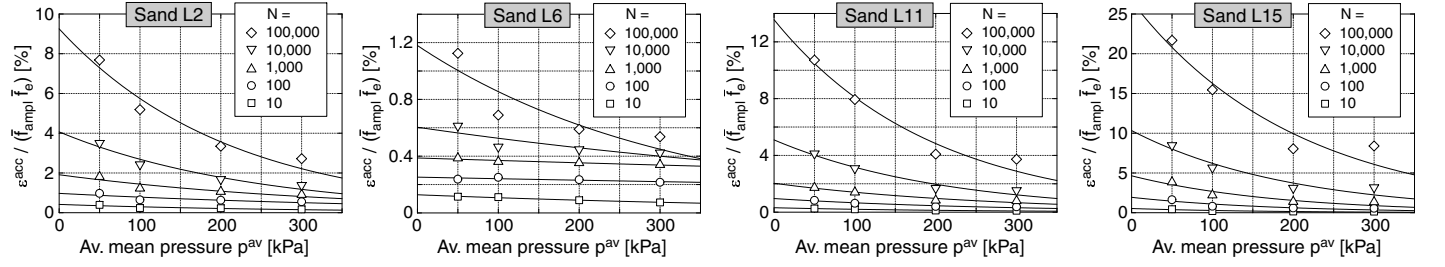


Figure 8. Accumulated strain $\varepsilon^{\text{acc}} / (\bar{f}_{\text{ampl}} \bar{f}_e)$ as a function of average mean pressure p^{av} (all tests: $\eta^{\text{av}} = 0.75$, $\zeta = q^{\text{ampl}}/p^{\text{av}}$).

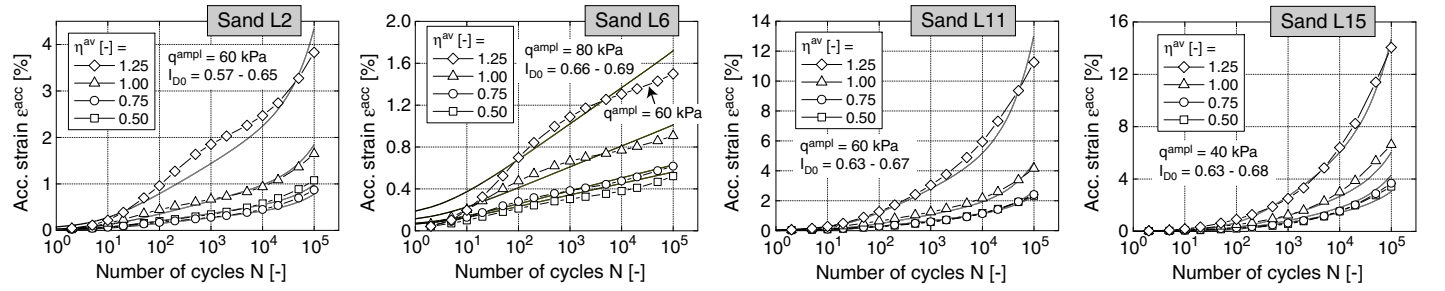


Figure 9. Accumulation curves $\varepsilon^{\text{acc}}(N)$ in tests with different average stress ratios \bar{Y}^{av} (all tests: $p^{\text{av}} = 200$ kPa), thick solid curves = recalculation with HCA model.

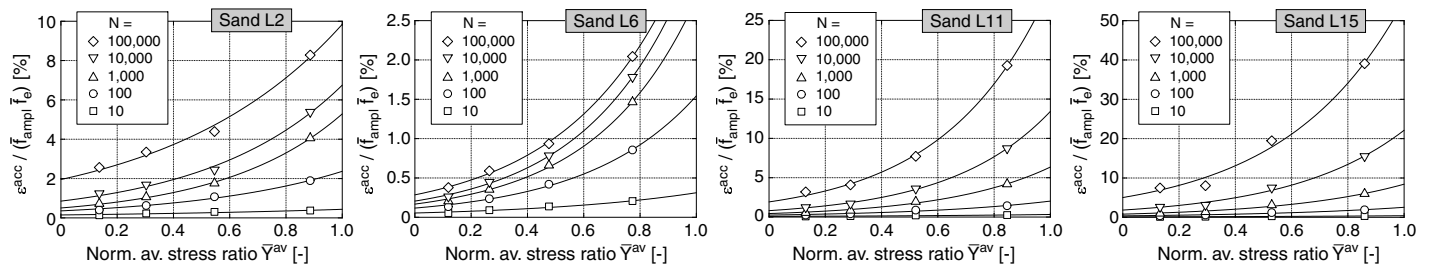


Figure 10. Accumulated strain $\varepsilon^{\text{acc}} / (\bar{f}_{\text{ampl}} \bar{f}_e)$ as a function of normalized average stress ratio \bar{Y}^{av} (all tests: $p^{\text{av}} = 200$ kPa).

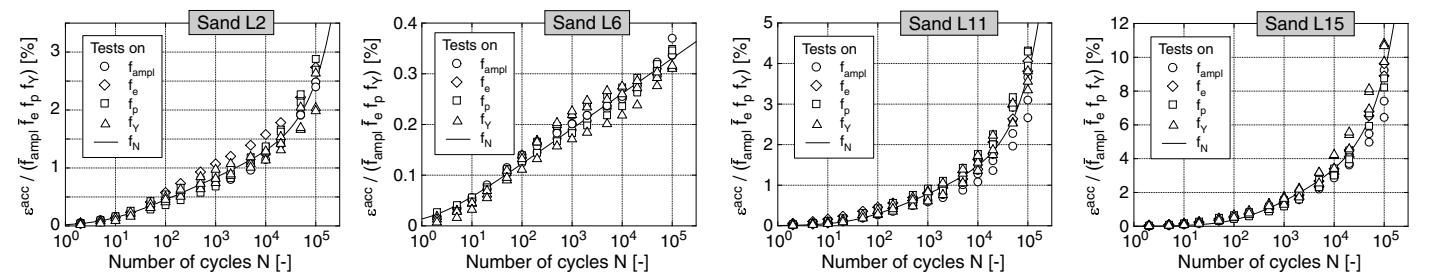


Figure 11. Curves $\varepsilon^{\text{acc}}(N) / (\bar{f}_{\text{ampl}} \bar{f}_e \bar{f}_p \bar{f}_Y)$, fitting of function f_N

Table 1. HCA model parameters for the 14 tested sands

Sand	e_{\min}	e_{\max}	"by hand" C_{ampl}	method			C++ program									
				C_e	C_p	C_Y	C_{N1}	C_{N2}	C_{N3}	C_{ampl}	C_e	C_p	C_Y	C_{N1}	C_{N2}	C_{N3}
	[-]	[-]	[-]	[-]	[-]	[-]	[10^{-4}]	[-]	[10^{-5}]	[-]	[-]	[-]	[-]	[10^{-4}]	[-]	[10^{-5}]
L1	0.634	1.127	1.60	0.60	0.40	1.84	5.61	0.328	8.79	1.69	0.60	0.40	1.99	0.485	0.30	10.5
L2	0.596	0.994	1.43	0.64	0.29	1.94	16.8	0.137	5.37	1.33	0.65	0.30	1.89	18.0	0.15	6.0
L3	0.591	0.931	1.76	0.59	0.69	2.72	10.5	0.185	2.02	1.85	0.61	0.55	3.00	8.25	0.24	2.1
L4	0.571	0.891	1.92	0.55	0.53	2.52	5.07	0.197	2.76	1.97	0.57	0.52	2.82	4.35	0.30	3.5
L5	0.580	0.879	1.77	0.52	0.29	2.77	2.77	0.303	1.86	1.84	0.54	0.32	3.14	2.50	0.54	2.0
L6	0.591	0.877	1.70	0.56	0.12	2.57	3.01	0.576	0	1.64	0.58	0.11	2.72	3.66	0.89	0.1
L7	0.626	0.817	1.46	0.51	0.11	3.49	1.41	0.907	0	1.48	0.51	0.09	3.49	1.28	0.96	0
L10	0.541	0.864	1.53	0.53	0.36	2.21	19.3	0.0439	5.74	1.67	0.53	0.32	2.37	13.4	0.075	5.5
L11	0.495	0.856	2.03	0.50	0.42	2.41	23.3	0.0257	8.18	2.43	0.53	0.50	2.89	15.4	0.040	13.5
L12	0.474	0.829	1.40	0.47	0.39	2.70	51.4	0.0131	7.74	1.60	0.48	0.44	3.02	36.0	0.016	10.5
L13	0.414	0.791	1.68	0.40	0.39	2.44	53.6	0.00969	6.85	1.85	0.40	0.34	3.12	26.6	0.0090	10.0
L14	0.394	0.749	2.06	0.32	0.66	2.67	46.6	0.00817	5.70	2.34	0.34	0.45	3.29	23.0	0.0065	7.5
L15	0.387	0.719	1.76	0.33	0.55	2.15	68.6	0.00732	6.67	1.97	0.34	0.44	2.69	41.2	0.0070	7.5
L16	0.356	0.673	1.36	0.31	0.23	1.99	107	0.00611	8.78	1.53	0.31	0.23	2.45	79.2	0.0050	8.0

$\varepsilon^{\text{acc}}(N)$ for the more well-graded sands show a bending in the semi-logarithmic scale, which becomes more pronounced with increasing coefficient of uniformity of the tested material (see L11 and L15 in Figure 11). These findings agree well with the results of the earlier study documented by Wichtmann et al. (2009). The parameters C_{N1} , C_{N2} and C_{N3} (columns 7 to 9 of Table 1) were received by fitting the data in Figure 11 with the function f_N (solid curve):

$$f_N = C_{N1} [\ln(1 + C_{N2} N) + C_{N3} N] \quad (6)$$

The loading frequency does not influence the rate of strain accumulation in non-cohesive soils (see the literature review given by Wichtmann et al. (2009)) and is thus not considered in the HCA model.

As an alternative to the "by hand" calibration outlined above, the HCA model parameters were also determined by means of a C++ program. It finds those parameters for which the sum of the squares of the differences between the experimentally obtained ε^{acc} -data and the data predicted by the HCA model takes its minimum. The method may be seen as some kind of "fine tuning" of the parameters. The parameters summarized in columns 10 to 16 of Table 1 differ from those calibrated "by hand" due to simplifications of the "by hand" method (for example mean values $\bar{\varepsilon}^{\text{ampl}}$ and \bar{e} are used in the diagrams, parameters determined for different N -values are averaged).

4 RE-CALCULATION OF ELEMENT TESTS

The parameters given in columns 10 to 16 of Table 1 were used for recalculations of the element tests with the HCA model. The predicted curves have been added as solid lines in Figures 2, 5, 7 and 9. The parameters determined "by hand" (columns 3 to 9 of Table 1) deliver quite similar curves. In most cases the deviation between the experimental and the calculated data is small, confirming the good prediction of the HCA model. For some sands slightly too low accumulation rates are predicted for small pressures (Figure 7) which is due to deficits of the function f_p . This will be inspected in more detail in future.

5 SIMPLIFIED CALIBRATION PROCEDURE

In Figure 12 the HCA model parameters are plotted versus mean grain size d_{50} , coefficient of uniformity C_u or minimum void ratio e_{\min} , respectively. The data from the tests described by Wichtmann et al. (2009) were re-analyzed with $C_{\text{ampl}} \neq 2.0$ and are included in Figure 12. The correlations defined by Equations (7) to (13) are given in Figure 12 as solid lines and may be used for a simplified estimation of a set of parameters.

The parameter C_{ampl} does not correlate with d_{50} or C_u (Figure 12a,b). For C_e both, a correlation with d_{50} and C_u (Figure 12c,d) and with minimum void ratio e_{\min} (Figure 12e) could be established. The values of C_p and C_Y plotted in Figure 12f-i were obtained calculating C_{ampl} and C_e from Equations (7) and (8). Similarly, the data for C_{N1} , C_{N2} and C_{N3} in Figure 12j-o have been analyzed with C_{ampl} , C_e , C_p and C_Y calculated from Equations (7) to (10). Beside the calibration methods discussed in Section 3, the parameters C_{ampl} , C_e , C_p and C_Y were also estimated from the rate data (see Wichtmann et al., 2010a). C_{N1} , C_{N2} and C_{N3} were determined both, from the data of all curves $\varepsilon^{\text{acc}}(N)$ and from the curves of the three tests with different amplitudes only. The poor correlation between C_{N3} and d_{50} can possibly be improved by means of data from tests with larger numbers of cycles ($N > 10^5$).

$$C_{\text{ampl}} = 1.70 \quad (7)$$

$$C_e = 0.95 \cdot e_{\min} \quad (8)$$

$$C_p = 0.41 \cdot [1 - 0.34 (d_{50} - 0.6)] \quad (9)$$

$$C_Y = 2.60 \cdot [1 + 0.12 \ln(d_{50}/0.6)] \quad (10)$$

$$C_{N1} = 4.5 \cdot 10^{-4} \cdot [1 - 0.306 \ln(d_{50}/0.6)] \cdot [1 + 3.15 (C_u - 1.5)] \quad (11)$$

$$C_{N2} = 0.31 \cdot \exp[0.39 (d_{50} - 0.6)] \cdot \exp[12.3(\exp(-0.77C_u) - 0.315)] \quad (12)$$

$$C_{N3} = 3.0 \cdot 10^{-5} \cdot \exp[-0.84 (d_{50} - 0.6)] \cdot [1 + 7.85 (C_u - 1.5)]^{0.34} \quad (13)$$

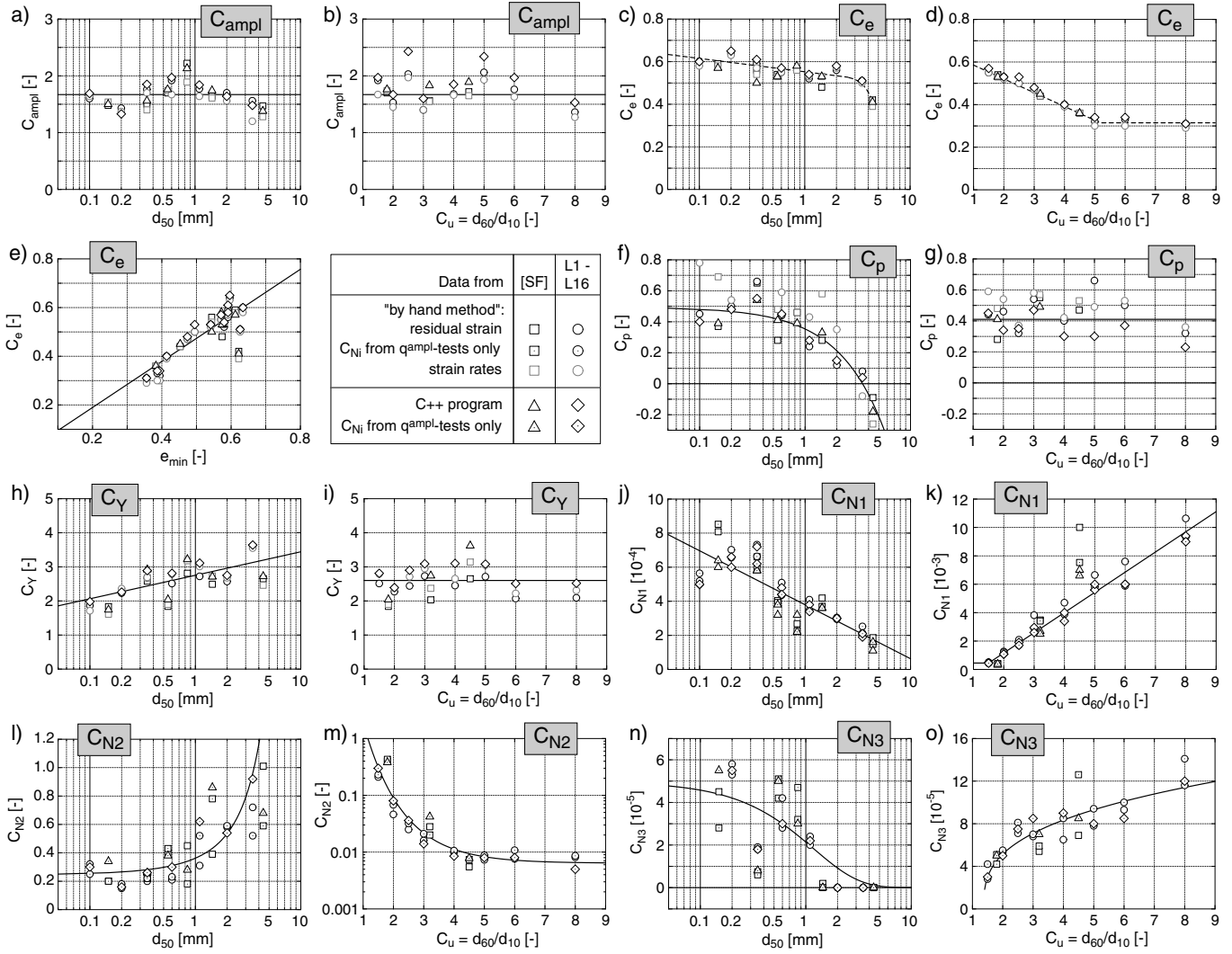


Figure 12. Correlations of the HCA model parameters with d_{50} , C_u or e_{min} , respectively (SF= Wichtmann et al., 2009)

6 SUMMARY, CONCLUSIONS AND OUTLOOK

Based on the data from approx. 350 drained cyclic triaxial tests performed on 22 quartz sands with different grain size distribution curves a simplified procedure for the determination of the parameters of the authors' high-cycle accumulation (HCA) model has been developed. Correlations of the HCA model parameters with mean grain size d_{50} , coefficient of uniformity C_u or minimum void ratio e_{min} , respectively, have been formulated. In future the simplified calibration procedure will be extended to granular materials with fines content.

7 ACKNOWLEDGEMENTS

The study presented in the paper has been performed in the framework of the project A8 of SFB 398 "Life-time oriented design concepts" during the former work of the authors at Ruhr-University Bochum, Germany. The authors are grateful to DFG (German Research Council) for the financial support and to M. Skubisch who carefully performed the cyclic triaxial

tests.

REFERENCES

- Niemunis, A., Wichtmann, T. & Triantafyllidis, T. 2005. A high-cycle accumulation model for sand. *Computers and Geotechnics*, 32(4):245-263.
- Wichtmann, T., Niemunis, A. & Triantafyllidis, T. 2009. Validation and calibration of a high-cycle accumulation model based on cyclic triaxial tests on eight sands. *Soils and Foundations*, 49(5): 711-728.
- Wichtmann, T., Niemunis, A. & Triantafyllidis, T. 2010a. On the determination of a set of material constants for a high-cycle accumulation model for non-cohesive soils. *Int. J. Numer. Anal. Meth. Geomech.*, 34(4):409-440.
- Wichtmann, T., Niemunis, A. & Triantafyllidis, T. 2010b. Towards the FE prediction of permanent deformations of offshore wind power plant foundations using a high-cycle accumulation model. In *International Symposium: Frontiers in Offshore Geotechnics, Perth, Australia*.